Research paper

Characterizing shocks from explosives with an optical fiber gauge

Jeremy E. Monat†, Joel R. Carney, V. H. Whitley, and G. I. Pangilinan

Research Department, Indian Head Division, Naval Surface Warfare Center 101 Strauss Avenue, Building 600, Indian Head, MD 20640, USA
†Corresponding address: jeremy.monat@navy.mil

Received: May 27, 2005 Accepted: December 9, 2005

Abstract

We present a gauge to characterize explosively-generated shocks in solids where traditional gauges are not applicable. The laser-pumped optical fiber gauge embedded in Modified Gap Test cylinders correctly determined the shock's arrival time and was sensitive to pressure. Although the gauge requires hydrocode modeling before quantitative pressure accuracy can be assessed, the gauge can qualitatively compare the performance of explosives.

Keywords: Optical fiber gauge, Explosive, Shock

1. Introduction

This paper describes the operation and usefulness of an optical fiber gauge for explosives scientists and engineers studying shocks generated in small-scale tests. This gauge uses changes in refractive index to measure shock time of arrival and is being developed for quantifying pressure.

Characterizing the shocks generated when explosives detonate is important to understanding their performance. Engineers prefer to minimize costs by evaluating explosives with small-scale tests. Consequently, gauges must be small, remotely operated, and immune to the electrical interference inherent in being so close to an electrically-initiated detonator. Although piezoelectric and piezoresistive gauges[1)~5)] can be quite thin, they are susceptible to electrical noise[6)]. Another proven gauge is the Velocity Interferometry System for Any Reflector (VISAR)[7)], but it is complex to operate and requires a reflective surface, so it cannot probe many geometries. Finally, the ruby gauge measures pressure and temperature under static[8)] and dynamic conditions[9)]. Ruby hemispheres on the tip of an optical fiber pumped by a laser can operate remotely[6)]. However, the requirement of a streak camera makes the technique expensive and complex. In summary, existing gauges are significantly limited for shock characterization.

To address these restrictions on shock characterization, we are developing a gauge based on light reflection at an interface. Termed the Gauge using Refractive Index for Pressure, or GRIP, it requires only a continuous-wave laser, an optical fiber, a photodiode, and an oscilloscope. In a test comparing the GRIP and a ruby gauge underwater, the GRIP agreed with the ruby gauge[10)].

Here, the Modified Gap Test (MGT) evaluated the GRIP's applicability to solids. We examined two applications: a thin layer of silicone on the fiber tip, and a boot of fluid surrounding the fiber. The first application's results might constitute a calibration curve, while the second application responded to the shock upon its arrival at the GRIP's tip. Both applications require hydrocode modeling for accurate conversion of the GRIP traces to pressures.

2. Experimental section

2.1 GRIP setup and principles

Figure 1 shows the GRIP's optoelectronic setup as previously described[10)]. An optical fiber guided 532 nm laser light into the test chamber, and a photodiode monitored the amount of light reflected from the optical fiber-substance interface. A simple model describes the measured signal:

$$S(t) = W\phi\left[\left(\frac{n_{subst}(t) - n_{fiber}}{n_{subst}(t) + n_{fiber}}\right)^2 + s_0\right] \qquad \text{Eqn. 1}$$

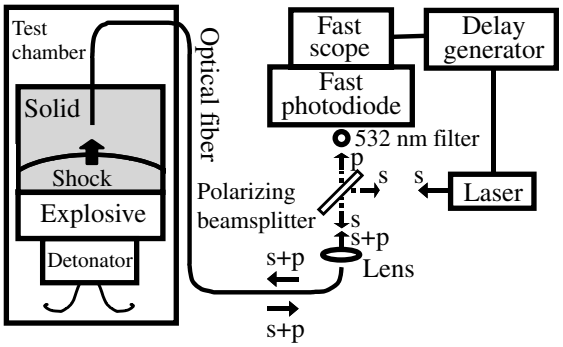

Fig. 1 Optoelectronic schematic for GRIP in Modified Gap Tests. The labels s and p refer to light polarizations. Because the polarizing beamsplitter reflects s-polarized light and transmits p-polarized light, polarization-sensitive detection reduces noise from scatter. The 532 nm bandpass filter prevents broadband emission from the explosion from reaching the photodiode detector.

where $S(t)$ (V) is the photodiode signal measured by the oscilloscope as a function of time, W (mW) is the laser power entering the optical fiber, ϕ (V mW^{-1}) is the overall conversion efficiency of light input into the optical fiber to voltage measured by the oscilloscope, $n_{subst}(t)$ is the refractive index of the substance at the optical fiber-substance interface as a function of time, n_{fiber} is the refractive index of optical fiber core, and s_0 is the background scattering fraction when no light is reflected from the optical fiber-substance interface itself. In this paper, interface refers to any step boundary of refractive index.

To determine the pressure of the substance in contact with the optical fiber tip, one must convert the GRIP trace to refractive index of the substance, and then to pressure. To calibrate refractive index vs. GRIP signal, we fit ϕ and s_0 to static GRIP signals for fluids of known refractive index as described previously[10]. Refractive index often increases linearly as density increases, as in the Gladstone-Dale model. In turn, density typically increases as pressure increases but decreases as temperature increases. A calibration curve of peak refractive index vs. Modified Gap Test shock pressure might then convert refractive index to pressure, assuming the substance's temperature is approximately the same between tests.

2.2 Modified gap tests

We followed the MGT protocol (see Fig. 2a) because it has been calibrated for peak shock pressure as a function of PMMA (polymethyl methacrylate, "plexiglass") gap distance[11)~13)]. An RP-80 detonator (Reynolds) initiated a cylindrical 50.8 mm diameter × 50.8 mm tall pentolite explosive charge, which subjected a PMMA cylinder directly above the pentolite to shock compression. The distance between the pentolite and GRIP's tip along the PMMA cylinder's axis defined the gap. Gaps from 23 to 52 mm corresponded to pressures from 6 to 2 GPa, respectively. Each optical fiber had a 0.400 mm diameter silica core (Fiberguide) and was cleaved by an automated cleaver (Vytran).

To verify MGT shock pressures, a framing camera (Imacon) measured shock velocities (see Section 3.1). A wooden baffle prevented debris ejected by the explosion from obscuring the PMMA cylinder. A flat window allowed light to pass through the PMMA unbent by a curved surface (see Fig. 3). Creating this window by removing material (0.4 mm in depth) from two opposite sides of the PMMA cylinder does not change the MGT calibration[11].

In the first GRIP application method, termed silicone on tip (see Fig. 2b), silicone rubber was the applied sensing medium. The silicone was designed to constitute the $n_{subst}(t)$[14] in Eqn. 1 when the silicone's density and refractive index changed during shock compression. A thin layer (approximately 0.1 mm) of clear colorless silicone rubber (Dow Corning 3145 RTV) on the fiber tip sufficed because the reflectance equation, incorporated in Eqn. 1, is valid for any layer thicker than half the wavelength of light

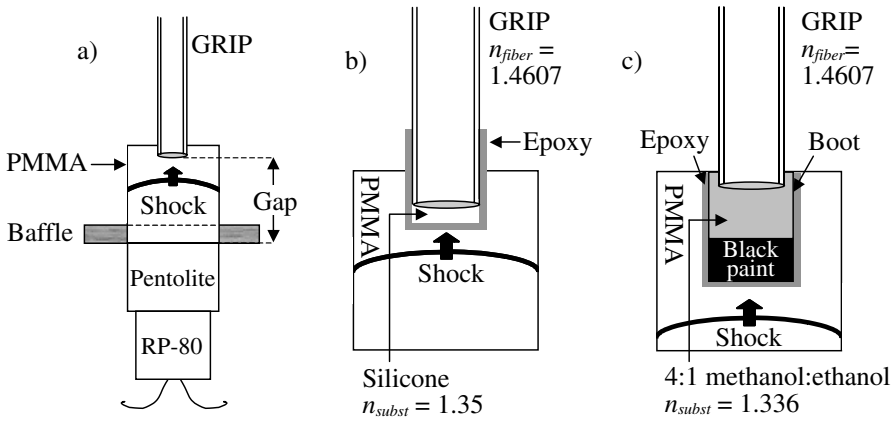

Fig. 2 a) Modified gap test setup for characterizing shocks. The gap is the distance between the top of the pentolite explosive charge and the tip of the GRIP optical fiber gauge inserted into the PMMA cylinder. b) Schematic of silicone on tip GRIP application. c) Schematic of boot of fluid GRIP application.

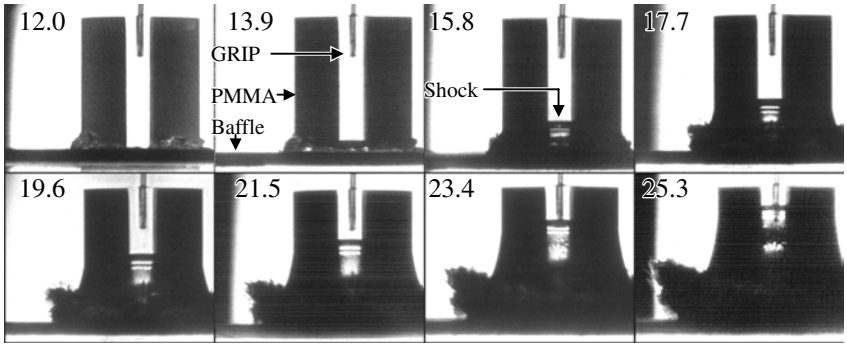

Fig. 3 Framing camera photographs for one typical MGT. The shock (uppermost dark front) moved up the PMMA cylinder towards the GRIP. The numbers are the times in μs following initiation of the detonator.

being used (herein, $\lambda / 2 = 266$ nm)[15]. We applied silicone under a microscope, allowed the silicone to cure overnight, then trimmed off excess silicone with a razor blade. A 0.99 mm diameter hole down the PMMA cylinder's axis housed the GRIP fiber, and ultraviolet (UV) cured epoxy held the fiber in place[16]. Because air bubbles within materials decrease the pressure of incident shocks due to impedance mismatches[17], we removed air bubbles before curing the epoxy.

The second GRIP application method, referred to as boot of fluid (see Fig. 2c), used a fluid as the sensing medium. We chose the pressure medium of 4:1 methanol:ethanol because it remains hydrostatic up to 10 GPa[18], has a known refractive index vs. pressure curve[19], and showed no visual change under static compression through 3.25 GPa. The boot was a polyethylene pipette with inner diameter approximately 1.4 mm and outer diameter approximately 2.5 mm. Black paint approximately 1 mm deep in the pipette's open end prevented light from reaching other interfaces[20]. After we cut off the pipette bulb and injected 4:1 methanol:ethanol into the pipette stem with a syringe and needle, we inserted the optical fiber. Then, with the assembly oriented vertically, UV light began curing the epoxy as it flowed into the top of the pipette. This was necessary because the uncured epoxy reacted with the 4:1 methanol:ethanol and formed an insoluble viscous substance, but the cured epoxy was inert. Next, we drilled a 2.8 mm diameter hole down the PMMA cylinder's axis and filled the hole with UV-curing epoxy. Finally, we removed air bubbles by allowing the epoxy to settle in the hole for an hour before we carefully inserted the boot assembly and cured the epoxy.

3. Results and discussion

3.1 Framing camera photography

Framing camera photographs verified MGT shock pressure. Figure 3 shows an example set of photographs; the shock is the uppermost dark front moving up the middle of the PMMA cylinder. After we computed the shock velocity, we used the Hugoniot of PMMA[12] to obtain particle velocity and pressure. The results agreed with the MGT calibration of pressure vs. distance, which confirmed that the setup used here reproduced the MGT protocol. The camera's spatial resolution dictated the uncertainty in shock position and velocity, which results in pressure uncertainties as shown by the pressure error bars

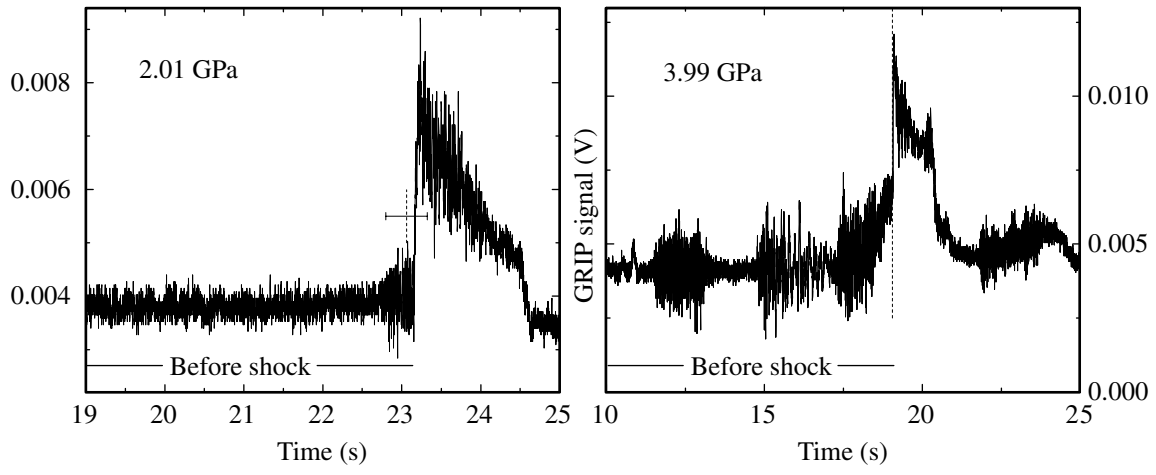

Fig. 4 GRIP traces from silicone on tip tests at two MGT pressures. Dashed vertical lines are the shock arrival times at the GRIP's tip according to the framing camera; the error bar is the uncertainty in the framing camera interpolation (for 3.99 GPa, the uncertainty is within the width of the dashed line).

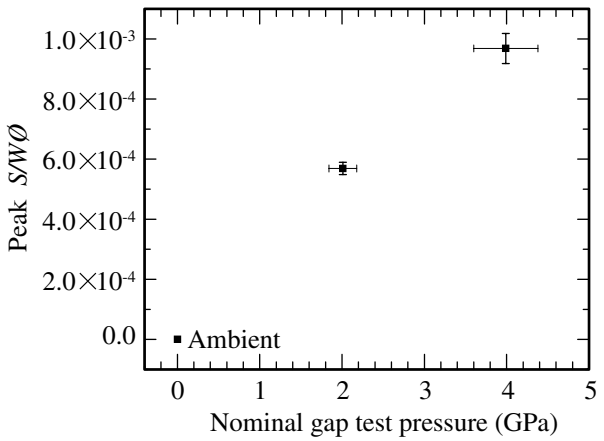

Fig. 5 Summary of peak of normalized GRIP traces vs. nominal MGT shock pressure for two silicone on tip MGT tests. Horizontal error bars are uncertainties in pressure calculated by the framing camera, and vertical error bars come from standard deviations in GRIP signals. Note the ambient-pressure point for comparison.

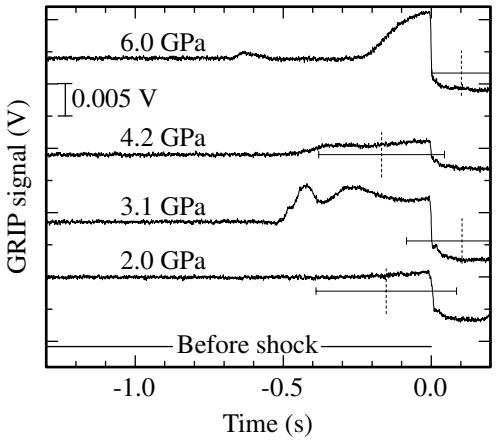

Fig. 6 GRIP traces from boot of fluid tests at four MGT pressures. Traces are vertically offset for clarity and horizontally shifted so the shock arrives at time zero according to the GRIP traces. Dashed vertical lines are the shock arrival times at the GRIP's tip according to the framing camera; the error bars are uncertainties in framing camera interpolations.

in Fig. 5. We also used the photographs with interframe times 0.8-2.1 μs to measure the shock arrival time at the GRIP's tip with an uncertainty of approximately 0.2-0.5 μs (we estimate interpolations are accurate to one-quarter of the interframe time).

3.2 GRIP traces

Figure 4 shows that the silicone on tip GRIP application correctly measured time of shock arrival with respect to the framing camera. Figure 4 labels each trace with its nominal MGT calibration[11)~13)] pressure: 2.01 GPa (51.6 mm gap) and 3.99 GPa (37.6 mm gap). These are the peak shock pressures PMMA experiences when the gap is composed solely of PMMA. The vertical dashed lines are the shock arrival times at the GRIP's tip according to the framing camera. These coincided within the camera's experimental uncertainty (shown as error bars) with the rapid increase in GRIP signal, demonstrating that the latter corresponded to the shock.

Additional interfaces complicated the analysis of Fig. 4 in terms of refractive index and pressure. Before the shock reached the GRIP, each GRIP trace held constant at its ambient-pressure value. If changes across only the fiber-silicone interface modulated these traces when the shock arrived, the traces would move downward upon shock compression when the silicone rubber became denser. Because the traces moved in the opposite direction, another interface (most likely silicone-epoxy) must have dominated the signal. In addition, shock compression may change the refractive index of the optical fiber core itself, changing n_{fiber} in Eqn. 1 and introducing another interface within the optical fiber. Because changes in the refractive index across multiple interfaces at pressure affected the traces, Eqn. 1 cannot convert the signal $S(t)$ to refractive index $n_{subst}(t)$. Therefore we analyzed the data as normalized signal $S(t) / W\phi$.

Figure 5 shows that the peak of the normalized GRIP trace increased with nominal MGT pressure for these two tests compared to ambient-pressure silicone. Adjacent averaging of 20 points smoothed the GRIP signal traces, providing the peak values shown. Such a plot might be used as a calibration curve to relate normalized signal to pressure if further tests follow this trend.

Figure 6 shows that the boot of fluid application also correctly measured shock arrival times with respect to the framing camera. Fig. 6 shows GRIP traces from four boot of fluid tests and labels each trace by nominal MGT calibration[11)~13)] pressure: 6.0 GPa (23 mm gap), 4.2 GPa (37 mm gap), 3.1 GPa (42 mm gap), and 2.0 GPa (51 mm gap). Each trace moved rapidly downward upon shock arrival at the GRIP's tip (shown as time zero)[21)]. These arrival times coincided with those from the framing camera (dashed vertical lines) within the camera's experimental uncertainty (shown as error bars), confirming the shock front caused each GRIP trace's rapid downward motion. Although the trace moved downward as expected when the shock arrived at the GRIP's tip, additional interfaces, particularly the shocked fiber-unshocked fiber interface, also complicated these traces.

Before the results can be converted to refractive indices or pressures, three-dimensional modeling is needed to account for pressures and temperatures across interfaces. A hydrocode description of the surrounding materials and their refractive indices will be addressed in the future. Nevertheless, the silicone on tip GRIP application can determine, using the MGT, which of two explosive charges produces a greater pressure at a given gap distance using normalized GRIP signal change (as in Fig. 5).

4. Conclusions

Using an optical fiber, the Gauge using Refractive Index for Pressure (GRIP) monitored shock fronts in Modified Gap Tests. We examined two GRIP applications: a thin layer of silicone rubber on the fiber tip, and a boot of fluid surrounding the fiber. The first application may be useful for empirically determining the peak signal vs. MGT pressure. In the second application, the GRIP responded to the shock when it reached the GRIP's tip. The GRIP is clearly useful as a shock time-of-arrival gauge even in opaque housings, in complex geometries, and under electrical interference where existing techniques fail. As Fig. 5 suggests, the silicone on tip GRIP application can compare explosive performance using the MGT by determining which of two explosive charges produces a greater pressure at a given gap distance. Consideration of additional interfaces and the response of materials, including the optical fiber, is necessary to employ the GRIP for refractive index and pressure measurements.

Acknowledgements

We thank Dr. Jared Gump for static pressure measurements, Robert Hay for technical assistance, and Dr. Jerry Forbes for helpful discussions. NAVSEA Indian Head In-House Laboratory Independent Research program and Lawrence Livermore National Laboratory provided funding.

References

1) M. A. Meyers, Dynamic Behavior of Materials, Wiley, New York (1994).
2) H. C. Vantine, L. M. Erickson, J. Janzen, J. Appl. Phys., 51, 1957 (1980).
3) B. Cunningham, K. S. Vandersall, A. M. Niles, D. W. Greenwood, F. Garcia, J. W. Forbes, W. H. Wilson, "Carbon Resistor Pressure Gauge Calibration at Low Stresses" in Shock Compression of Condensed Matter-2001, edited by M. D. Furnish, N. N. Thadhani and Y. Horie, American Institute of Physics, Melville, N.Y. (2002), p. 1137.
4) D. Greenwood, J. Forbes, F. Garcia, K. Vandersall, P. Urtiew, L. Green, L. Erickson, "Improvements in the Signal Fidelity of the Manganin Stress Gauge" in Shock Compression of Condensed Matter-2001, edited by M. D. Furnish, N. N. Thadhani and Y. Horie, American Institute of Physics, Melville, N.Y. (2002), p. 1157.
5) F. Bauer, "Behavior of Ferroelectric Ceramics and PVF_2 Polymers Under Shock Loading" in Shock Waves in Condensed Matter-1981, edited by W. J. Nellis, L. Seaman and R. A. Graham, American Institute of Physics, New York (1982), p. 251.
6) G. I. Pangilinan, T. P. Russell, M. R. Baer, J. Namkung, P. Chambers, Appl. Phys. Lett., 77, 684 (2000).
7) S. A. Sheffield, D. D. Bloomquist, C. M. Tarver, J. Chem. Phys., 80, 3831 (1984).
8) J. D. Barnett, S. Block, G. J. Piermarini, Rev. Sci. Instrum., 44, 1 (1973).
9) P. D. Horn, Y. M. Gupta, Phys. Rev. B, 39, 973 (1989).
10) J. E. Monat, J. R. Carney, G. I. Pangilinan, "Novel Optical Fiber-Based Gauge for Measuring Transient Pressures" in Shock Compression of Condensed Matter-2003, edited by M. D. Furnish, Y. M. Gupta and J. W. Forbes, American Institute of Physics, Melville, N.Y. (2004), p. 1281.
11) T. P. Liddiard, Jr., D. Price, Recalibration of the Standard Card-Gap Test, Naval Ordnance Laboratory, White Oak, NSWC TR 65-43 (1965).
12) J. O. Erkman, D. J. Edwards, A. R. Clairmont, Jr., D. Price, Calibration of the NOL Large Scale Gap Test; Hugoniot Data for Polymethyl Methacrylate, Naval Ordnance Laboratory, White Oak, NOLTR 73-15 (1973).
13) T. P. Liddiard, J. W. Forbes, A Summary Report of the Modified Gap Test and the Underwater Sensitivity Test, Naval Surface Warfare Center, Dahlgren, NSWC TR 86-350 (1987).
14) J. Staudenraus, W. Eisenmenger, Fortschritte der Akustik-DAGA '92, 301 (1992).
15) E. Hecht, Optics (2nd edition), Addison-Wesley, Reading, Massachusetts (1987).
16) After we embedded the GRIP in the MGT cylinder, laser light entered the fiber, passed through the silicone layer, reflected off one or more subsequent interfaces (the silicone-epoxy interface likely contributed, see section 3.2), and recoupled into the fiber. Attempts to prevent such reflections by coating the silicone layer with black paint failed because the laser light decomposed the paint.
17) S. A. Sheffield, R. L. Gustavsen, M. U. Anderson, "Shock Loading of Porous High Explosives" in High-Pressure Shock Compression of Solids IV, edited by L. Davison, Y. Horie and M. Shahinpoor, Springer-Verlag, New York (1997), p. 23.
18) G. J. Piermarini, S. Block, J. D. Barnett, J. Appl. Phys., 44, 5377 (1973).
19) J. H. Eggert, L.-w. Xu, R.-z. Che, L.-c. Chen, J.-f. Wang, J. Appl. Phys., 72, 2453 (1992).
20) In this case, the laser did not decompose the paint because the paint was further away from the fiber tip. As a result, the laser light exiting the fiber diverged enough to lower the laser's power density at the black paint below its decomposition threshold.
21) Laser light reflecting off the shock front likely caused the increase in traces before 0 μs; see J. E. Monat, J. R. Carney, V. H. Whitley, G. I. Pangilinan, Shock Compression of Condensed Matter-2005, American Institute of Physics, in press.